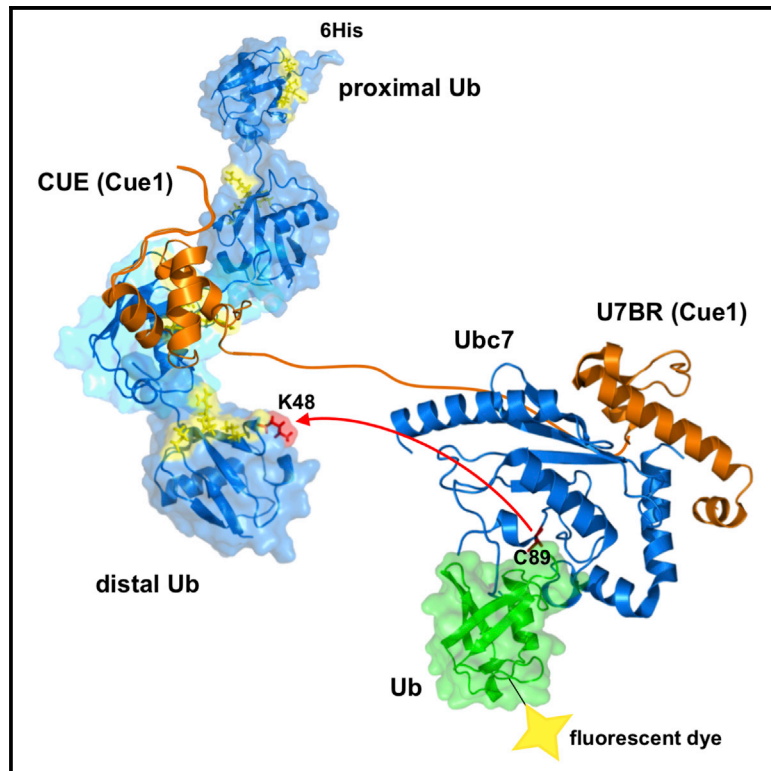


# Molecular Cell

## The CUE Domain of Cue1 Aligns Growing Ubiquitin Chains with Ubc7 for Rapid Elongation

### Graphical Abstract



### Authors

Maximilian von Delbrück,  
Andreas Kniss, Vladimir V. Rogov, ...,  
Peter Güntert, Thomas Sommer,  
Volker Dötsch

### Correspondence

tsommer@mdc-berlin.de (T.S.),  
vdoetsch@em.uni-frankfurt.de (V.D.)

### In Brief

Synthesizing polyubiquitin chains poses an intriguing steric problem because the distance between substrate and elongation site constantly increases. von Delbrück et al. show that the CUE domain of Cue1 overcomes this problem by positioning the growing chain relative to the E2 enzyme and accelerates the elongation process as part of ERAD.

### Highlights

- The CUE domain of Cue1 adopts a non-canonical structure
- The CUE domain accelerates K48-linked ubiquitin chain elongation in the ERAD process
- The ubiquitin moiety next to the acceptor ubiquitin is the preferred interaction site
- Impaired binding of the CUE domain delays degradation of the ERAD substrate Ubc6

### Accession Numbers

2MYX



# The CUE Domain of Cue1 Aligns Growing Ubiquitin Chains with Ubc7 for Rapid Elongation

Maximilian von Delbrück,<sup>1,5</sup> Andreas Kniss,<sup>2,5</sup> Vladimir V. Rogov,<sup>2</sup> Lukas Pluska,<sup>1</sup> Katrin Bagola,<sup>4</sup> Frank Löhr,<sup>2</sup> Peter Güntert,<sup>2</sup> Thomas Sommer,<sup>1,3,\*</sup> and Volker Dötsch<sup>2,\*</sup>

<sup>1</sup>Max-Delbrück-Center for Molecular Medicine in the Helmholtz Association, Robert-Rössle-Strasse 10, 13125 Berlin-Buch, Germany

<sup>2</sup>Institute of Biophysical Chemistry and Center for Biomolecular Magnetic Resonance, Goethe University, Max-von-Laue Strasse 9, 60439 Frankfurt am Main, Germany

<sup>3</sup>Institute for Biology, Humboldt Universität zu Berlin, Invalidenstrasse 43, 10115 Berlin, Germany

<sup>4</sup>Ludwig Institute for Cancer Research, University of Oxford, Old Road Campus Research Building, Oxford OX3 7DQ, UK

<sup>5</sup>Co-first author

\*Correspondence: [tsommer@mdc-berlin.de](mailto:tsommer@mdc-berlin.de) (T.S.), [vdoetsch@em.uni-frankfurt.de](mailto:vdoetsch@em.uni-frankfurt.de) (V.D.)

<http://dx.doi.org/10.1016/j.molcel.2016.04.031>

## SUMMARY

Ubiquitin conjugation is an essential process modulating protein function in eukaryotic cells. Surprisingly, little is known about how the progressive assembly of ubiquitin chains is managed by the responsible enzymes. Only recently has ubiquitin binding activity emerged as an important factor in chain formation. The Ubc7 activator Cue1 carries a ubiquitin binding CUE domain that substantially stimulates K48-linked polyubiquitination mediated by Ubc7. Our results from NMR-based analysis and *in vitro* ubiquitination reactions point out that two parameters accelerate ubiquitin chain assembly: the increasing number of CUE binding sites and the position of CUE binding within a growing chain. In particular, interactions with a ubiquitin moiety adjacent to the acceptor ubiquitin facilitate chain elongation. These data indicate a mechanism for ubiquitin binding in which Cue1 positions Ubc7 and the distal acceptor ubiquitin for rapid polyubiquitination. Disrupting this mechanism results in dysfunction of the ERAD pathway by a delayed turnover of substrates.

## INTRODUCTION

Ubiquitination is a crucial post-translational modification involved in many cellular processes. Ubiquitin molecules are transferred to client proteins through the concerted actions of ubiquitin-activating enzymes (E1), ubiquitin-conjugating enzymes (E2), and ubiquitin ligases (E3). Ubiquitin itself can be targeted for ubiquitination on seven internal lysine residues and on its N terminus, resulting in the assembly of polymeric chains. Distinct chain types do not only display different topologies (Komander and Rape, 2012) but are also associated with divergent signaling output. For instance, polyubiquitin chains linked

via K48 represent the major signal for proteasomal degradation (Thrower et al., 2000), whereas K63-linked chains mediate widespread nonproteasomal functions such as DNA repair, transcriptional activation, endocytosis, or protein trafficking (Conaway et al., 2002; Haglund and Dikic, 2005; Huang and D'Andrea, 2006; Chen and Sun, 2009). These various polyubiquitin chains are decoded into cellular responses by ubiquitin binding domains (UBDs) that guide effector proteins to ubiquitinated substrates (Weissman, 2001). UBDs specifically distinguish between different polyubiquitin molecules by recognizing the linkage and length of chains. Monoubiquitin is bound by UBDs with a  $K_D$  in the micromolar range, whereas polyubiquitin chains provide multiple binding surfaces, thus increasing binding affinity (Husnjak and Dikic, 2012).

In contrast to this well-known deciphering function of UBDs, the function of ubiquitin binding in polyubiquitin chain formation is poorly understood. For instance, the activities of the E2 enzymes Ubc13 (Pastushok et al., 2005), Ube2g1 (Choi et al., 2015), and Cdc34 (Choi et al., 2010) rely on ubiquitin binding events. In addition, it has already been shown that processive polyubiquitin chain formation can be promoted by noncovalent interactions of ubiquitin with the backside of certain E2 enzymes (Brzovic et al., 2006; Buetow et al., 2015) as well as by RING domains showing ubiquitin binding activity (Brown et al., 2014; Wright et al., 2016). Furthermore, E4 enzymes have been identified that recognize ubiquitinated proteins and elongate the attached ubiquitin chains (Koegl et al., 1999).

A recent report on polyubiquitination activity in the endoplasmic reticulum (ER)-associated protein degradation (ERAD) pathway revealed that the UBD of Cue1, the coupling of ubiquitin conjugation to ER degradation (CUE) domain, stimulates ubiquitin chain formation (Bagola et al., 2013). Cue1 contains a C-terminal Ubc7 binding region (Kostova et al., 2009; Bazirgan and Hampton, 2008) recruiting Ubc7 to the ER membrane (Biederer et al., 1997) for activation (Metzger et al., 2013). Ubc7 acts together with different ERAD RING finger ubiquitin ligases such as HRD1, DOA10, and the Asi complexes (Bays et al., 2001; Kreft et al., 2006; Khmelinskii et al., 2014; Foresti et al., 2014). Substrate proteins are then polyubiquitinated and subsequently

**Table 1. Structural Statistics of the CUE Domain of Cue1**

NOE Assignment <sup>a</sup>	
Completeness of resonance assignment (%) <sup>a</sup>	99.2
Total number of NOESY crosspeaks	3,264
Assigned NOESY crosspeaks	3,090
Conformational Restraints	
Total NOE distance restraints	1,605
Short range $ i-j  \leq 1$	704
Medium range $1 <  i-j  < 5$	440
Long range $ i-j  \geq 5$	461
Dihedral angle restraints ( $\phi/\psi$ )	92
Hydrogen bonds	18
Structure Statistics	
CYANA target function value ( $\text{\AA}^2$ ) <sup>b</sup>	$1.11 \pm 0.04$
AMBER energies (kcal/mol) <sup>c</sup>	$-2764 \pm 66$
Restraint Violations <sup>c</sup>	
Max. distance restraint violation ( $\text{\AA}$ )	0.13
Number of violated distance restraints $> 0.2 \text{\AA}$	0
Max. dihedral angle restraint violations ( $^\circ$ )	2.01
Number of violated dihedral angle constraints $> 5^\circ$	0
Ramachandran Plot	
Residues in most favored regions (%)	86.8
Residues in additionally allowed regions (%)	12.6
Residues in generously allowed regions (%)	0.6
Residues in disallowed regions (%)	0.0
Root-Mean-Square Deviation (RMSD) (Residues 63–114)	
Average backbone RMSD to mean ( $\text{\AA}$ )	$0.20 \pm 0.03$
Average heavy atom RMSD to mean ( $\text{\AA}$ )	$0.49 \pm 0.05$
NOESY, nuclear Overhauser and exchange spectroscopy; CYANA, combined assignment and dynamics algorithm for NMR applications; AMBER, assisted model building with energy refinement.	
<sup>a</sup> For the non-labile $^1\text{H}$ and the backbone $\text{H}^N$	
<sup>b</sup> Before restrained energy minimization	
<sup>c</sup> After energy minimization with the program OPALp	

removed from the ER membrane by an ERAD-specific Cdc48 complex. Subsequently, target proteins are escorted by adaptor proteins to the proteasome in the cytosol.

Although polyubiquitin signals play essential roles in many cellular pathways, the molecular basis on how they are generated remains elusive. In contrast to single attachments of ubiquitin to a substrate, building a ubiquitin chain challenges the E1-E2-E3 cascade with multiple conjugation events at the same molecule. This sequential assembly is a spatially dynamic process in which the distal tip of a growing chain constantly changes its relative position to the active site in the E2-E3 complex. In consequence, chain assembly slows down with increasing chain length, as shown, for example, for the anaphase promoting complex (APC)/cyclosome (C) E3 complex (Meyer and Rape, 2014; Wickliffe et al., 2011). To circumvent this problem, auxiliary factors may facilitate chain assembly, and ubiquitin binding domains appear to be the key to this process. Here we provide a detailed molecular mechanism of how a UBD stimulates ubiquitin polymerization. We demonstrate that the CUE

domain of Cue1 accelerates the elongation of chains by specific binding events that coordinate the spatial arrangement of the E2 Ubc7 with the distal end of nascent chains.

## RESULTS

### Helices $\alpha 1$ and $\alpha 3$ of the CUE Domain Bind the Hydrophobic Patch of Ubiquitin

So far, structural studies of the yeast protein Cue1 have been limited to the Ubc7 binding region (U7BR) (Metzger et al., 2013). The importance of the CUE domain for K48-linked ubiquitin chain formation raised the question of how ubiquitin binding and ubiquitin chain elongation are functionally connected (Bagola et al., 2013). As a starting point, we used nuclear magnetic resonance (NMR) spectroscopy to determine the structure of the CUE domain (Table 1). This analysis unveiled a compact three-helical bundle characteristic for CUE and UBA domains (Figure 1A). Unlike canonical CUE domains, the CUE domain of Cue1 requires a C-terminal extension that bears two phenylalanine residues for stable folding (Figure 1A; Figures S1A–S1F). In particular, F108 is an essential part of the hydrophobic core (Figure S1C).

To study the interactions between the CUE domain and ubiquitin in more detail, we performed NMR titration experiments with  $^{15}\text{N}$ -labeled CUE domain and unlabeled ubiquitin (Figures S2A–S2E). Chemical shift perturbations (CSPs) revealed that the most affected residues of CUE are located in the transition of helix  $\alpha 1$  to the adjacent  $\alpha 1\alpha 2$  loop (V73, L76, A77, and N79) and in helix  $\alpha 3$  (E96, E100, and L103) (Figure 1B). The LAP<sup>76–78</sup> motif corresponds to the strictly conserved MFP motif of other CUE domains. Quantitative analysis of the peak positions yielded a  $K_D$  of  $152 \pm 5 \mu\text{M}$  (Figure S2E). Using a reverse experimental setup, we mapped the interaction surface on ubiquitin (Figure 1B). Titration of  $^{15}\text{N}$ -labeled ubiquitin with unlabeled CUE domain unveiled that binding involves the hydrophobic patch of ubiquitin centered around amino acids L8–I44–V70 and further includes R42, G47, and L71. Notably, the interaction surface on ubiquitin is in close proximity to the K48 residue without K48 directly contributing to binding (Figure 1C).

Based on the chemical shift perturbation pattern, we calculated a structural model of the CUE/ubiquitin complex using the software package HADDOCK (de Vries et al., 2010). This model supports a significant contribution of R42 in ubiquitin for the interaction with E100 of CUE (Figure 1C). At the same time, this structural arrangement ensures that K48 of ubiquitin is accessible for further chain elongation (Figure S2F).

### Fluorescence-Based Analysis of Ubiquitin Chain Elongation Reactions

Knowing the binding properties of the CUE domain, we tried to understand how an interaction with ubiquitin stimulates ubiquitin chain formation by Ubc7. Therefore, we developed a fluorescence-based assay that allowed us to precisely follow elongation reactions of ubiquitin chains. Different chains of defined linkage and length were used as ubiquitin acceptors. These model substrates were blocked at their C termini to prevent charging onto enzymes. The elongation of chains by single fluorescently labeled ubiquitin molecules was monitored using

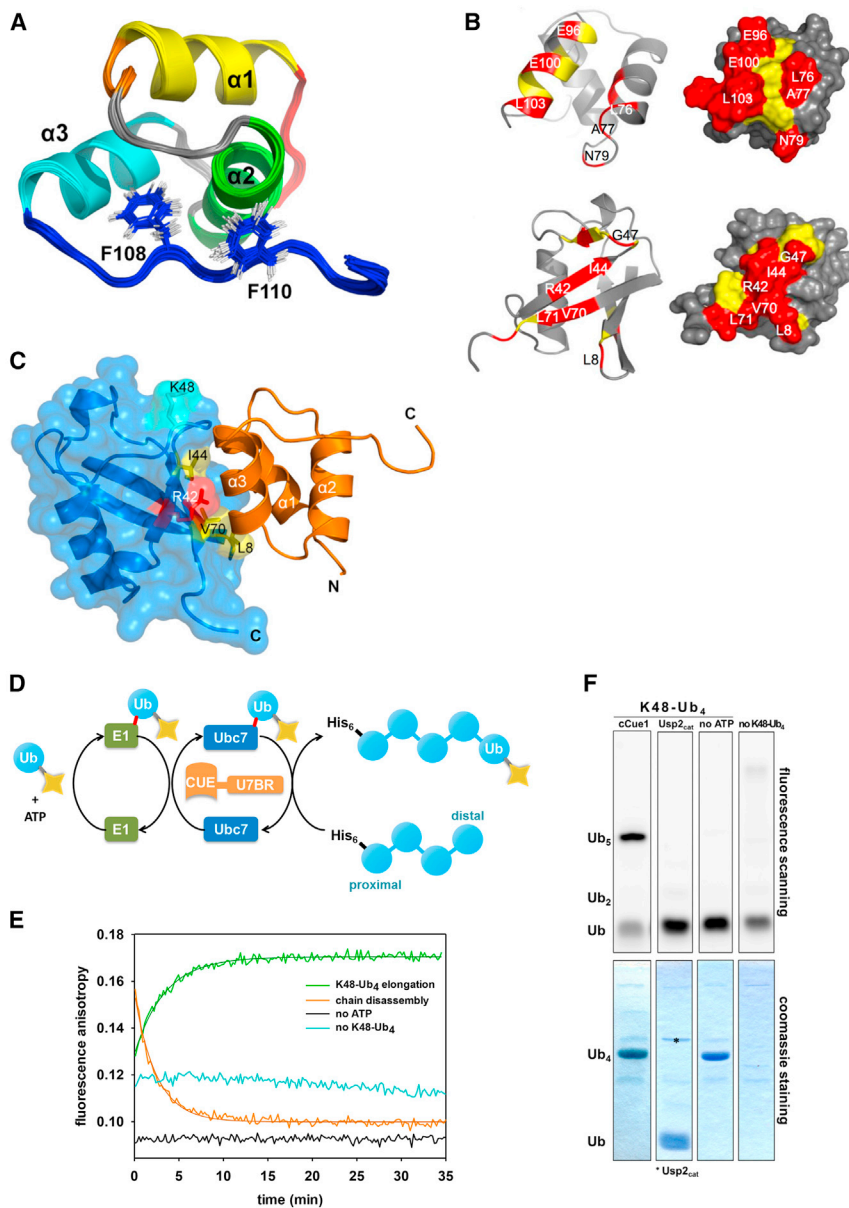


**Figure 1. The Interaction of the CUE Domain with Ubiquitin and Fluorescence Anisotropy-Based Analysis of Ubiquitin Chain Elongation Reactions**

(A) Superposition of the NMR solution structure (PDB: 2MYX) ensemble comprising the 20 lowest-energy conformers. The three  $\alpha$  helices are colored in yellow, green, and cyan (from the N to the C terminus), whereas the structured regions following and preceding the three helices are colored in blue (C-terminal extension) and red (N-terminal extension). The LAP motif is highlighted in orange. See also Figure S1.

(B) Mapping of affected residues upon binding onto the structure of the CUE domain and ubiquitin (PDB: 1UBQ). The structures are shown as a ribbon diagram as well as a surface representation. Residues shifting more than 0.12 ppm are colored in yellow and residues shifting more than 0.18 ppm in red for Cue1. For ubiquitin, residues shifting more than 0.13 ppm are shown in yellow, whereas residues shown in red shifted more than 0.22 ppm. See also Figure S2.

(C) Model of the CUE/ubiquitin complex. The highest-scored structural model from a CSP-based HADDOCK structure calculation is shown. The structure reveals the importance of R42 of ubiquitin for complex formation. CUE is bound in close proximity to the K48 residue, the site of further chain conjugation; however, K48 itself remains completely accessible.

(D) Ubiquitin chains are elongated *in vitro* by one ubiquitin. Because of a C-terminal His<sub>6</sub> tag, pre-assembled chains only serve as an acceptor for ubiquitin. Fluorescently labeled ubiquitin is activated by the E1 enzyme and transferred to the E2 enzyme Ubc7. In concert with the cytosolic fragment of Cue1 (cCue1), Ubc7 elongates ubiquitin chains that are employed in excess. The RING domain of Hrd1 (cHrd1) is optionally added to facilitate the reaction. See also Figure S3.

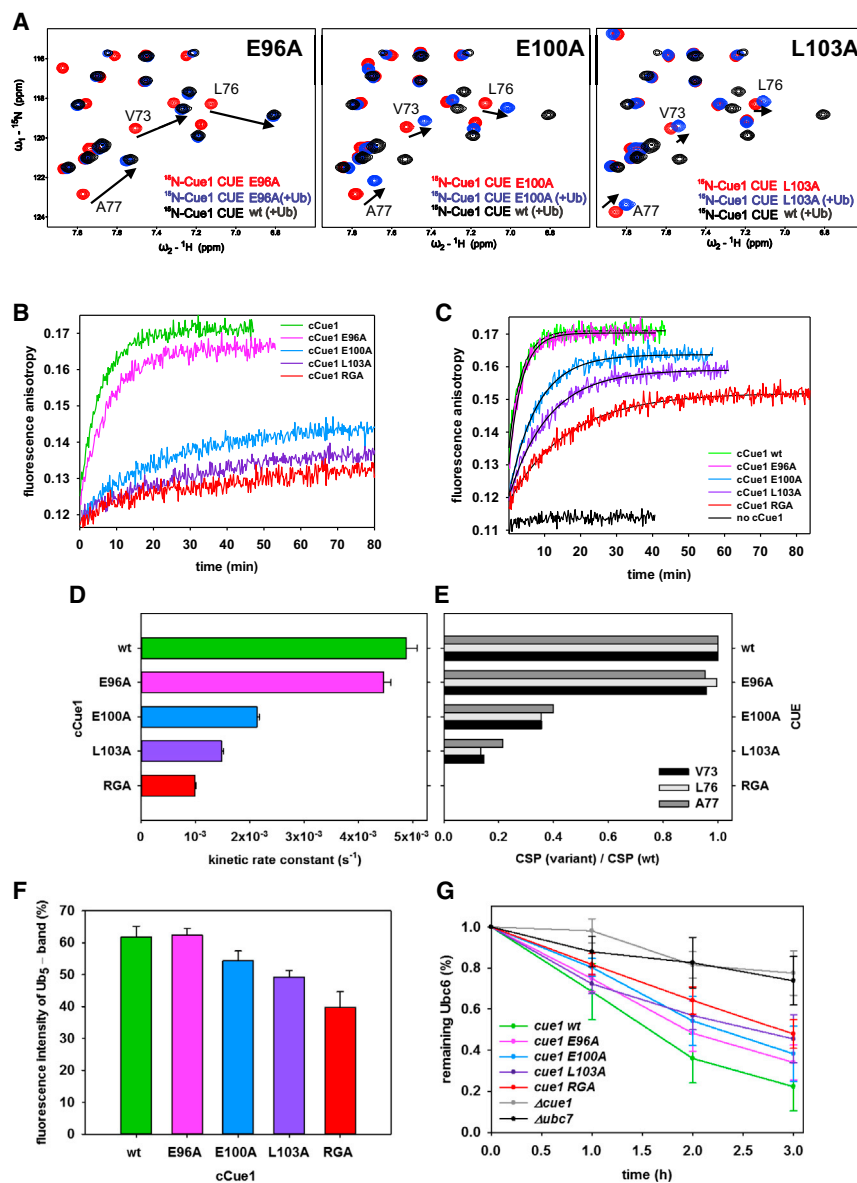
(E) In fluorescence anisotropy measurements a rising signal monitors the elongation of K48-linked tetraubiquitin (green line). After subsequent addition of a deubiquitinating enzyme (Usp2<sub>cat</sub>), anisotropy signals decrease (orange line) close to the baseline of reactions omitting ATP (black line). Reactions lacking ATP or preassembled ubiquitin chains (blue line) do not show an increase in anisotropy.

(F) The yield of elongation products was determined by SDS-PAGE, fluorescence scanning, and Coomassie staining. Added Usp2<sub>cat</sub> is marked with an asterisk.

fluorescence anisotropy. In elongation experiments with tetraubiquitin, the signal increased because of a slower tumbling of the formed pentaubiquitin compared with labeled monoubiquitin (Figures 1D and 1E). This change in fluorescence anisotropy is strictly dependent on ATP. After subsequent addition of a deubiquitinating enzyme (Usp2<sub>cat</sub>), ubiquitin chains were completely disassembled, and fluorescence anisotropy decreased to its original level. Reactions lacking preassembled chains did not show a rise in signal. In addition, elongation of tetraubiquitin was pursued by quantifying the fluorescence intensities of the

reaction product pentaubiquitin by applying gel electrophoresis (Figure 1F; Figure S3B). Both experimental approaches yielded equivalent kinetics (Figure S3A), supporting fluorescence anisotropy measurements to be a robust and precise tool to monitor chain elongation. Reaction catalysis additionally required an E1 enzyme (Ube1), the yeast E2 enzyme Ubc7, and the soluble fragment of Cue1 (cCue1, residues 25–203), which encompasses both the CUE domain and the U7BR. Some experiments included the cytosolic fragment of the E3 enzyme Hrd1 (cHrd, residues 325–551) containing the RING finger domain.





### Ubiquitin Binding Affinity Correlates with Kinetics of Chain Elongation and Substrate Degradation

In the absence of cCue1, chain elongation by Ubc7 was strongly impeded (Figure 2B). This observation can be attributed to the missing activation of the E2 enzyme by the U7BR (Metzger et al., 2013). To investigate the effect of the CUE domain on polyubiquitination, the structurally important LAP<sup>76–78</sup> motif was replaced by RGA<sup>76–78</sup> (cCue1 RGA; Bagola et al., 2013), which results in an unfolded CUE domain (Figure S1F). Consistent with previously published data, reactions containing cCue1 RGA were substantially impaired in chain elongation (Figure 2B). In the presence of wild-type cCue1, elongation of K48-linked tetraubiquitin (K48-Ub<sub>4</sub>) was 5-fold faster than in the absence of a functional CUE domain, as indicated by the kinetic rate constants (Figure 2D). In line with this acceleration, the presence

### Figure 2. The Ubiquitin Binding Affinity of the CUE Domain Correlates with the Kinetics of Ubiquitin Chain Elongation Reactions In Vitro and the Degradation of the ERAD Substrate Ubc6 In Vivo

(A) Superposition of a section of [<sup>15</sup>N, <sup>1</sup>H]-HSQC spectra recorded for CUE variants E96A, E100A, and L103A in the presence (8-fold molar excess of ubiquitin, blue spectrum) and absence of ubiquitin (red spectrum). As a reference, the spectrum recorded for the wild-type CUE domain in the presence of the same amount of ubiquitin is shown (black spectrum) (see also Figure S4). Binding of the E96A variant resembles the wild-type protein, whereas variants E100A and L103A show diminished affinities. Substitutions in the LAP motif (L76R, A77G, and P78A) (cCue1 RGA) result in an unfolded CUE domain (Figure S1F) and prevent an interaction with ubiquitin.

(B and C) Fluorescence anisotropy traces were obtained from K48-Ub<sub>4</sub> elongation reactions with Ubc7 and cCue1 (green line) or cCue1 variants (E96A, pink line; E100A, blue line; L103A, purple line; and RGA, red line) in the presence (B) or absence of cHrd1 (C). Solid lines show mono-exponential fits of the data points on which basis kinetic parameters were calculated.

(D) Rate constants of elongation reactions of tetraubiquitin with cCue1 or the variants in (B).

(E) CSPs of representative residues (V73, L76, and A77) upon ubiquitin binding. Obtained shifts at an 8-fold molar excess of ubiquitin are compared between wild-type and CUE domain variants. The ratio between the CSPs observed for the wild-type CUE domain and its variants was calculated.

(F) The yield of assembled elongation product pentaubiquitin of the reactions in (B) is calculated by the ratio of fluorescent pentaubiquitin over non-conjugated, fluorescently labeled monoubiquitin.

(G) Quantification of a cycloheximide-based decay assay of Ubc6 performed in the presence of the Cue1 variants (Figure S4C). The kinetics of degradation are color-coded as in (B). The quantities of variant proteins were similar throughout the experiments. Remaining amounts of Ubc6 from  $\Delta$ cue1 and  $\Delta$ ubc7 strains (data from a separate experiment) provide a baseline and indicate maximal delay of Ubc6 degradation.

of a functional CUE domain increased the yield of elongation product (Figure 2F). Chain elongation did not require cHrd1 but was facilitated by addition of the RING domain (Figures 2B and 2C). The U7BR-bound Ubc7 has an increased affinity for its cognate E3 RING domain, which, in turn, promotes the discharge of ubiquitin from E2, thereby driving ubiquitination (Metzger et al., 2013).

To investigate whether ubiquitin binding of the CUE domain directly correlates with the propensity of Cue1 to enhance chain elongation, we substituted amino acids in the UBD involved in this interaction. These variants (E96A, E100A, and L103A) retained the CUE fold but weakened ubiquitin binding affinity, as determined by NMR titration experiments (Figures 2A and 2E; Figures S4A and S4B). Although the E96 side chain does not contribute to ubiquitin recognition, the binding activity was decreased for the

E100A and even more for the L103A variant (as seen from the NMR titration experiments). Testing these cCue1 variants in elongation reactions with tetraubiquitin revealed a consistent correlation between binding affinities and kinetic rate constants. Wild-type cCue1 ( $[4.87 \pm 0.20] \times 10^{-3} \text{ s}^{-1}$ ) and the E96A variant ( $[4.46 \pm 0.13] \times 10^{-3} \text{ s}^{-1}$ ) exhibited comparable elongation kinetics. In contrast, reactions containing variants E100A ( $[2.13 \pm 0.05] \times 10^{-3} \text{ s}^{-1}$ ) and L103A ( $[1.48 \pm 0.03] \times 10^{-3} \text{ s}^{-1}$ ) were 2- to 3-fold slower (Figure 2D). Accordingly, the total amount of the reaction product pentaubiquitin was reduced (Figure 2F). Similar effects on elongation kinetics were observed regardless of whether cHrd1 was present or absent (Figure 2C). Finally, we analyzed the Cue1 variants *in vivo*, addressing polyubiquitin-mediated protein degradation. Ubc6 is a substrate of the DOA10 ubiquitin ligase complex and, as such, degraded by proteasomes in a Cue1/Ubc7-dependent manner (Bagola et al., 2013). In line with a slower assembly of ubiquitin chains because of weaker ubiquitin binding, the L103A Cue1 variant delayed the degradation of Ubc6 in yeast, whereas the other variants had less pronounced effects (Figure 2G). Complete absence of Cue1 or Ubc7 had a strong effect because, in both cases, the conjugating activity was missing. Thus, a rapid elongation of ubiquitin chains by Ubc7 relies on specific ubiquitin binding events by the CUE domain of Cue1 and seems to be required for the efficient degradation of some ERAD substrates.

#### Ubiquitin Chains with K48 Linkages and Growing Length Are Preferentially Elongated by cCue1/Ubc7

Ubc7 exclusively assembles K48-linked polyubiquitin on substrates *in vivo* (Ravid and Hochstrasser, 2007; Choi et al., 2015) and unanchored ubiquitin chains *in vitro* (Bagola et al., 2013). A substrate protein does not seem to be essential for polyubiquitination activity. Elongation reactions of monoubiquitin provide further evidence for a self-contained E2 system with the task to extend ubiquitin chains. All experiments with cCue1/Ubc7 and ubiquitin chains revealed a stimulation of elongation because of the CUE domain. This is in contrast to reactions with monoubiquitin that show no enhancing effect of the UBD (Figure 3A).

To evaluate this function, we applied ubiquitin chains of different linkage and length as substrates in our fluorescence-based assay. Additionally, we examined whether changes in the kinetics of chain elongation would correlate with differences in the binding affinities of the CUE domain by surface plasmon resonance (SPR) and NMR experiments. In line with a modestly stronger interaction with K48-linked chains (Figures S5A–S5D), we observed preferential elongation of K48- over K63-linked substrates (Figures 3B and 3C; Figures S5E–S5G). Distal elongation of the latter model substrate was ensured by K48R substitutions in all positions except at the distal ubiquitin. Besides the linkage type of a substrate, its size also influenced the elongation rate (Figure 3B). Increasing chain length accelerated elongation kinetics in the presence of the CUE domain, which can be explained by higher local concentrations of Ubc7 in the surrounding chains because of more binding sites. This effect is again modestly more pronounced for K48-linked chains than for K63-linked substrates, corresponding to the higher affinity of CUE to K48-linked ubiquitin.

cCue1 RGA was employed in kinetic analyses to evaluate the capability of U7BR-bound Ubc7 to elongate chains. Without a functional CUE domain, reactions with cCue1/Ubc7/cHrd1 were remarkably slow (Figures 3D and 3F; Figures S5H–S5J). In line with the general constraint of polyubiquitination lacking auxiliary ubiquitin binding events (Meyer and Rape, 2014; Wickliffe et al., 2011), elongation was decelerated with increasing chain length, an effect more pronounced for K48- than for K63-linked chains. Next we determined the degree of acceleration caused by the CUE domain to assess its function in chain elongation. The CUE domain-specific factor is set as the ratio of kinetic rate constants from reactions with wild-type cCue1 to reactions with cCue1 RGA and attained higher values for K48-linked chains than for K63-linked chains (Figure 3E). Moreover, the acceleration increased from K48-linked di- to tetraubiquitin, which was not observed for K63-linked chains. In summary, these results indicate that the CUE domain of Cue1 progressively accelerates the elongation of K48-linked chains with increasing length, counteracting the inability of Ubc7 to rapidly elongate growing chains.

#### CUE Binds the Proximal Moiety of K48-linked Diubiquitin with Higher Affinity Than the Distal Molecule

To understand why the CUE domain shows a small but significant preference for K48-linked chains, we synthesized K48- and K63-linked diubiquitin containing  $^{15}\text{N}$ -labeled moieties at either the proximal or distal position. Upon titration with unlabeled CUE domain, binding events at one of both positions could be analyzed. Chemical shift perturbations suggested that the interfaces of interaction with Cue1 are similar on mono- and diubiquitin (Figures 4A–4D). However, we observed one interesting difference between the associations with K63- and K48-linked diubiquitin. The latter displayed an additional interaction event involving position G75 at the C terminus of the distal ubiquitin moiety. Because the K48 residue of ubiquitin is in close proximity to the CUE binding site, this additional interaction specifically results from K48-linked monomers. Employing a binding model assuming two different binding sites in diubiquitin, we quantitatively analyzed NMR titration experiments and calculated  $K_D$  values (Figures 4E and 4F; Figure S6). In K48-Ub<sub>2</sub>, the CUE domain preferentially binds proximal ubiquitin ( $84 \pm 8 \mu\text{M}$ ), approximately 2-fold tighter than distal ubiquitin ( $151 \pm 13 \mu\text{M}$ ). In contrast, no difference in affinity for distal and proximal binding was detected for K63-linked diubiquitin ( $\sim 100 \mu\text{M}$ ; Figure 4F). Interestingly a previous study has presented similar binding analyses involving the CUE domain of the mammalian ERAD E3 gp78, revealing a preference for the distal moiety in K48- and K63-linked diubiquitin (Liu et al., 2012), reflecting a different organization in this ubiquitin ligase.

#### CUE Domain Binding Adjacent to the Distal Acceptor Ubiquitin Promotes Chain Elongation

Finally, we wanted to know whether the influence of the interaction of Cue1 with K48-linked ubiquitin molecules on chain elongation is position-dependent. Thus, we introduced the amino acid exchange R42A in either moiety of diubiquitin (Figure 5A). Monoubiquitin R42A displays reduced binding to the CUE domain ( $K_D = 600\text{--}700 \mu\text{M}$ ; Figure 3C). When placed in the distal molecule that serves as an acceptor for ubiquitin conjugation,

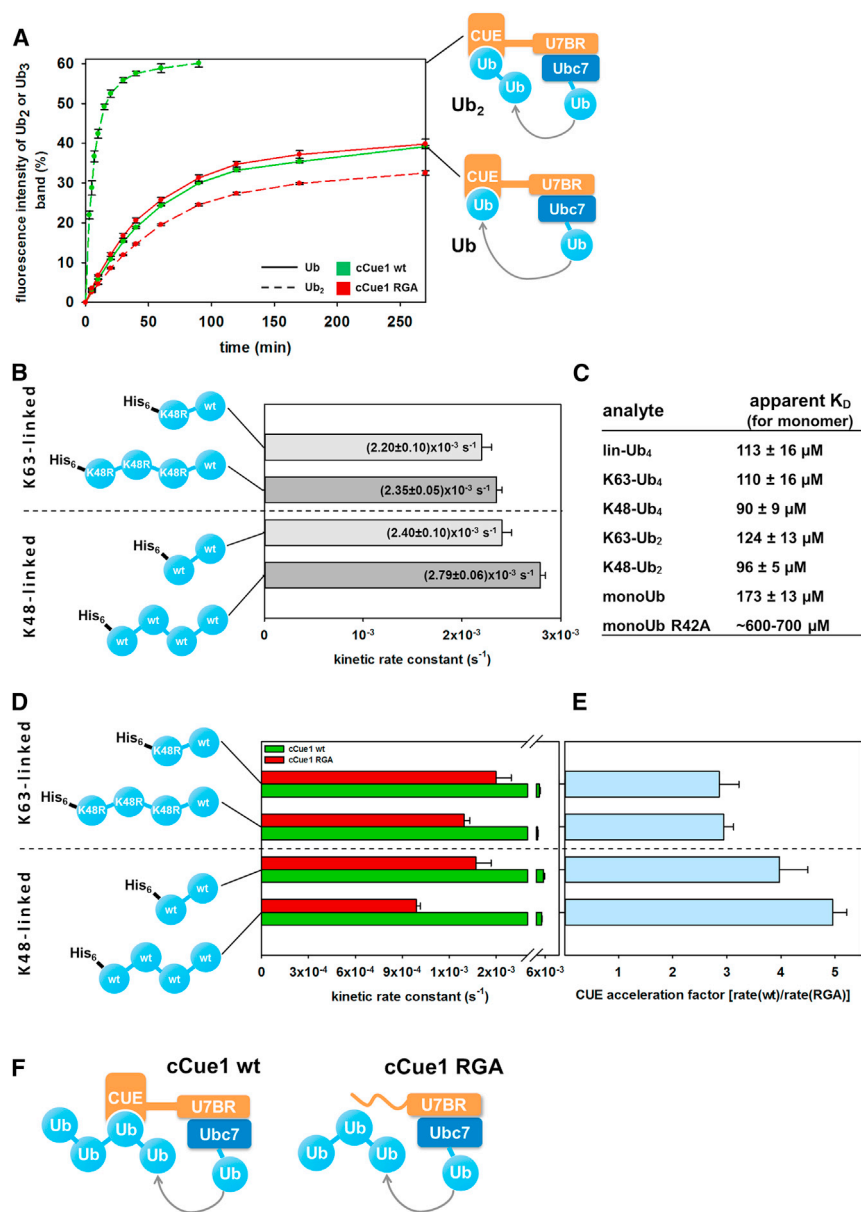


**Figure 3. The CUE Domain of Cue1 Preferentially Binds K48-linked Ubiquitin Chains and Stimulates Their Elongation**

(A) Kinetics of monoubiquitin (solid line) and diubiquitin (dashed line) elongation by Ubc7 and cCue1 (green lines) or cCue1 RGA (red lines) monitored by time-course experiments. The CUE domain stimulates elongation of ubiquitin chains but not of monoubiquitin.

(B) Kinetic rate constants of elongation reactions with cCue1 and Ubc7 for a set of ubiquitin chains linked via K48 or K63 (Figures S5E–S5J). K63-linked model substrates are restricted for distal elongation by K48R ubiquitin variants except at the distal moiety. Reactions accelerate from top to bottom, with K48-Ub<sub>4</sub> elongated fastest.

(C)  $K_D$  values for the interaction between the CUE domain and different ubiquitin chains were calculated from SPR binding data assuming a 1:1 binding model with multiple, independent, and equal binding sites.

(D) Kinetic rate constants of elongation reactions with Ubc7, cHrd1, and cCue1 (green bars) or cCue1 RGA (red bars) are shown in comparison for different substrate chains.

(E) Acceleration factors that quantify the CUE-specific stimulation were calculated as a ratio of kinetic rate constants of reactions with wild-type Cue1 and rate constants of reactions with Cue1 RGA (blue bars). The stimulating effect of the CUE domain is most pronounced for K48-linked chains and rises with increasing chain length for this linkage type.

(F) A working model of cCue1/Ubc7 illustrates ubiquitin chain elongation in the presence and absence of the CUE domain's binding activity.

the R42A variant had a negligible effect on elongation kinetics. In contrast, R42A at the proximal position reduced elongation in rate and efficiency. These findings suggest that binding of Cue1 to the proximal ubiquitin adjacent to the acceptor site promotes polyubiquitination. Elongation experiments of these diubiquitin molecules in the presence of cCue1 RGA exhibited almost identical reaction kinetics, indicating that the observed position effect is CUE domain-specific. Moreover, the UBD stimulated reactions in the presence of cHrd1, implying that Cue1 acts as a prevalent scaffold for ubiquitin chains (Figure S7A).

We now wondered how CUE binding within longer chains affects the elongation kinetics. K48-Ub<sub>4</sub> variants with single R42A amino acid exchanges in different ubiquitin moieties feature an equal number of binding sites and enabled us to map the action profile of the CUE domain. Again, analysis

of chain elongation kinetics yielded the most pronounced effect by introducing the R42A variant adjacent to the distal acceptor ubiquitin (Figure 5B; Figures S7B and S7D). For this substrate, the slowest elongation reaction was observed (~70% of the wild-type rate constant). Introducing multiple R42A ubiquitin variants in Ub<sub>4</sub> decelerated elongation even further (Figure 5C; Figures S7C and S7E). These data suggest that binding of cCue1 to any moiety within the chain accelerates the elongation reaction. However, the degree of stimulation depends on the position of the interaction within a chain, showing the highest effect when placed next to the acceptor ubiquitin. This effect is independent of linkage type and can also be measured for K63-linked diubiquitin (Figure S7F), suggesting that interaction with the ubiquitin molecule next to the acceptor site provides the optimal steric arrangement for Ubc7-based chain elongation.

To validate the importance of the position effect, we restricted CUE-ubiquitin interactions to certain positions within a chain. Therefore, we chemically crosslinked the single cysteine variant of cCue1 (T66C, C147S) with different ubiquitin (T9C) moieties (Figure S7G). Crosslinking cCue1 to the proximal moiety in

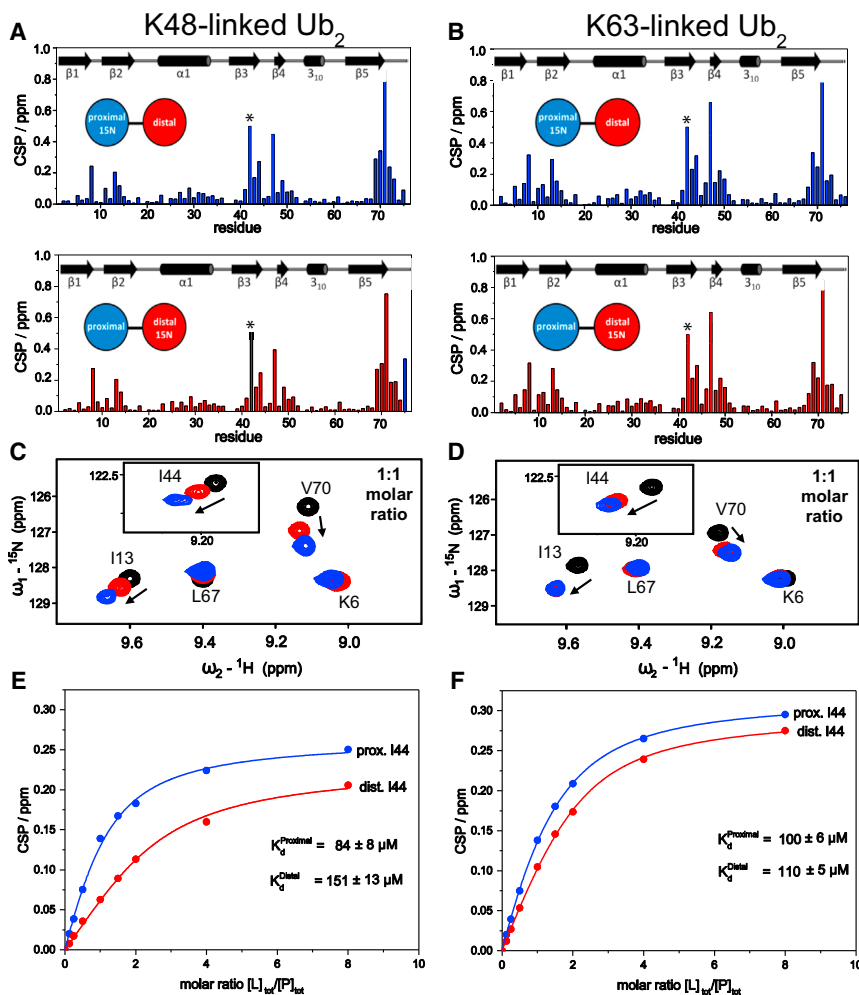


**Figure 4. The CUE Domain Preferentially Binds the Proximal Moiety in K48-linked Diubiquitin**

(A) Backbone amide CSP mapping of <sup>15</sup>N-labeled proximal ubiquitin or <sup>15</sup>N-labeled distal ubiquitin in K48-Ub<sub>2</sub> upon titration with unlabeled CUE domain. Proximal ubiquitin and the resulting CSPs are colored blue and distal ubiquitin and the corresponding CSPs red. Because the backbone amide signal of R42 disappeared, the indicated CSP of R42 was set to the arbitrary value of 0.5 to emphasize its importance in mediating CUE recognition. The CSP of G75 in distal ubiquitin is colored in blue because we propose that this represents an additional interaction with proximally bound CUE.

(B) The same data as in (A) for K63-Ub<sub>2</sub>.

(C) Overlay of a representative section of the [<sup>15</sup>N, <sup>1</sup>H]-HSQC spectra showing the unbound form of proximal/distal ubiquitin in black and the spectra recorded at a 1:1 molar ratio of CUE:Ub<sub>2</sub> either with proximally (blue) or distally (red) <sup>15</sup>N-labeled samples. Larger shifts for proximal ubiquitin indicate a significantly higher population of proximally bound CUE.

(D) The same overlays as in (C) for K63-Ub<sub>2</sub>. CUE interactions with proximal and distal ubiquitin of K63-Ub<sub>2</sub> are similar.

(E and F) Determination of K<sub>d</sub> values from the CSP data. The data were fitted assuming a binding model with two independent but different binding sites. The fit reveals a 2-fold increase in affinity for proximal K48-linked ubiquitin (E), while for K63-linked diubiquitin, similar affinities are obtained (F). See also Figure S6.

diubiquitin showed a drastic increase in the rate and efficiency of chain elongation (Figure 5D). Chain elongation was slower when cCue1 was crosslinked to the proximal position in triubiquitin. In contrast, crosslinking to the distal position of diubiquitin had an inhibitory effect. This strong acceleration of chain elongation by crosslinking to the positions adjacent to the acceptor site supports our model.

## DISCUSSION

Shaping a ubiquitin chain represents an intriguing steric problem. The longer a chain grows, the larger is the distance to the active center of the involved E2-E3 ligase complex. In a stochastic process, the growth of ubiquitin chains should slow down with increasing length of a chain. This general constraint in polyubiquitin formation has been reported previously (Meyer and Rape, 2014; Wickliffe et al., 2011). It is consistent with our kinetic measurements of the E2 Ubc7 activity missing a functional UBD. Here we present a mechanism of how the presence of the CUE domain in Cue1 counteracts this effect by directing Ubc7 to acceptor lysine residues at a distal ubiquitin molecule of a nascent ubiquitin chain. This leads to a progres-

sively accelerated elongation reaction with increasing chain length.

Corresponding to the K48-linkage specificity of Ubc7 (Bagola et al., 2013), CUE features a modestly stronger binding to K48-linked ubiquitin assemblies than to other chain types. The preference is caused by additional interactions at the C terminus of the neighboring ubiquitin molecules in these chains. In consequence, linked moieties in a chain are bound 2-fold stronger than the distal one. Furthermore, we observed an unconventional binding interface compared with consensus CUE domains. K48 of ubiquitin is excluded from the binding interface with Cue1, whereas, for instance, the CUE domain of Cue2 directly involves K48, thus potentially blocking it for further modifications (Kang et al., 2003). The accessibility of this lysine residue is a prerequisite for chain formation by Ubc7. Consistent with the binding preference, K48-linked chains are elongated faster than K63-linked model substrates in the presence of the CUE domain. However, because the Ubc7 system within ERAD is based solely on K48-linked chains, there was no evolutionary pressure to optimize the system for K48 versus K63 linkage types, explaining the relatively small differences observed for the interaction of the CUE domain with both chain



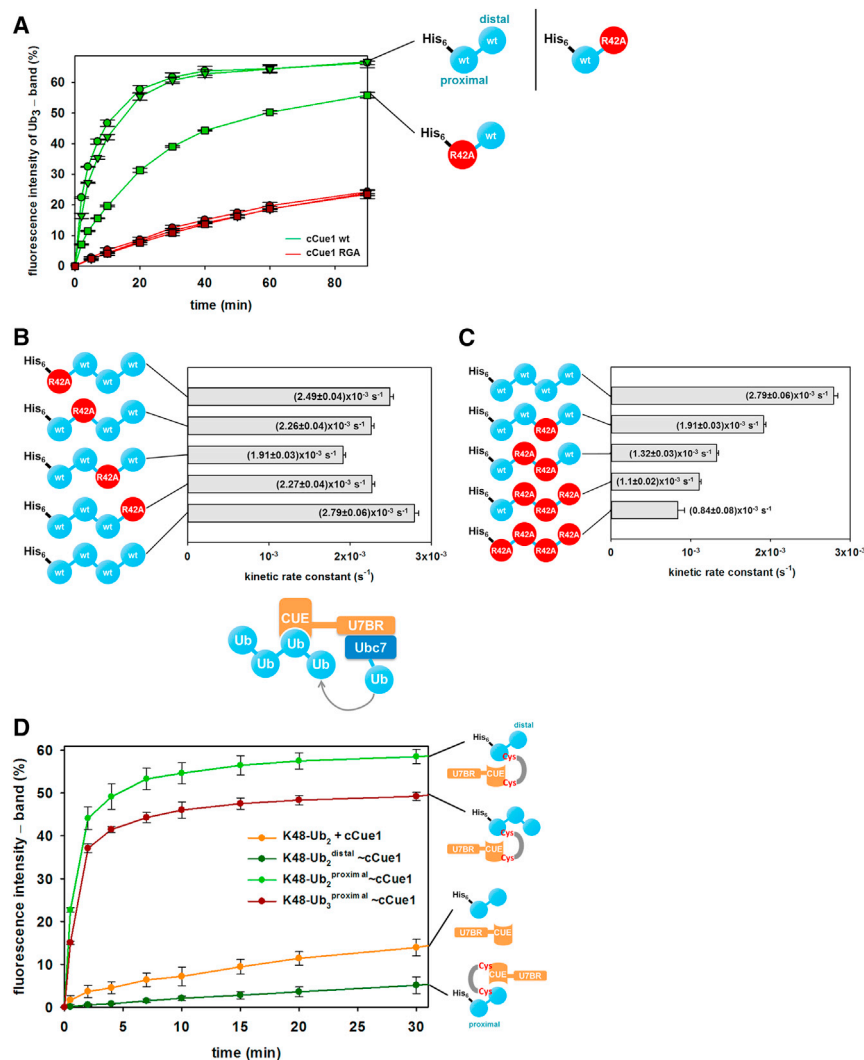


**Figure 5. An Interaction of the CUE Domain with the Moiety Adjacent to the Distal Acceptor Ubiquitin Strongly Promotes Chain Elongation**

(A) Elongation of diubiquitin catalyzed by Ubc7 and cCue1 (green lines) or cCue1 RGA (red lines) was followed by time-course experiments. The kinetics of reactions with wild-type diubiquitin (circles) and a variant with distal R42A ubiquitin (inverted triangles) were similar in the presence of cCue1. In contrast, the elongation of diubiquitin containing a proximal R42A ubiquitin was significantly decelerated (squares). Reactions with this set of diubiquitin molecules and cCue1 RGA exhibited almost identical kinetics.

(B) Kinetic rate constants of elongation reactions with cCue1, Ubc7, and K48-Ub<sub>4</sub> variants bearing single R42A ubiquitin molecules (Figures S7B and S7D). Deceleration of chain elongation is most pronounced for R42A that is located in the moiety adjacent to the distal acceptor ubiquitin. cCue1 binding at this position in tetraubiquitin as well as distal chain elongation by Ubc7 are depicted schematically in our working model.

(C) Kinetic rate constants of reactions with cCue1, Ubc7, and K48-Ub<sub>4</sub> variants that contain multiple R42A substitutions. An increasing number of substitutions progressively decelerates elongation kinetics (Figures S7C and S7E).

(D) Elongation reactions with cCue1 T66C C147S crosslinked to Ub T9C, which is placed at different positions in ubiquitin chains, are monitored by time-course experiments. Crosslinking cCue1 to the distal position of K48-linked diubiquitin (K48-Ub<sub>2</sub><sup>distal</sup>~cCue1, dark green line) strongly decelerates elongation. cCue1 fixed at proximal sites of diubiquitin (K48-Ub<sub>2</sub><sup>proximal</sup>~cCue1, light green line) or triubiquitin (K48-Ub<sub>3</sub><sup>proximal</sup>~cCue1, red line) yields fast kinetics. Reactions without crosslinking were performed with equimolar amounts of cCue1 and K48-Ub<sub>2</sub> (orange line) as a reference. See also Figures S7F and S7G.

assemblies. In summary, CUE binding converts an inherent decelerating chain formation by Ubc7 into a self-accelerating process.

Based on our kinetic analysis, we suggest two major factors increasing the pace of chain assembly. First, the number of binding sites: reducing the number of binding sites by introducing specific variants into ubiquitin chains or the CUE domain decelerates elongation reactions. This also includes the acceptor ubiquitin moiety and strongly indicates that multiple interactions of Cue1 with a ubiquitin chain increases the local concentration of Ubc7, which, in turn, promotes chain elongation.

Second, the position of CUE binding: deficient binding to the ubiquitin moiety adjacent to the distal end of a chain has a greater effect on the rate of chain assembly than at other positions. In addition, crosslinking of cCue1 with ubiquitin at this position enhanced chain elongation most. An interaction of Cue1 with the penultimate ubiquitin in a chain most likely orients Ubc7 to the distal end of a ubiquitin chain to productively transfer ubiquitin from the charged E2 to the acceptor lysine of the distal moiety. Binding to ubiquitin further away from the distal end

shows diminished stimulation because of increasing distance from the ubiquitin acceptor molecule.

In comparison with a recently reported mode of chain formation described in cell cycle control, our proposed mechanism seems to be perfectly adapted to rapid proteolytic processes of substrates with diverse biophysical properties, as in the case of the ERAD system (Kelly et al., 2014). The APC/C is a tightly adjusted system for regulatory degradation of cell cycle protagonists and simultaneously coordinates the recognition and ubiquitination of a limited pool of defined substrates. Here, the RING domain increases the affinity of the E2 Ube2S to the distal ubiquitin molecule, whereby chain elongation is enhanced. Tracking the end of chains is a stimulating effect that subsides with increasing chain length. ERAD challenges ubiquitin ligases with a much wider range of target proteins, although not all ERAD substrates seem to depend on the presence of a CUE domain (Bagola et al., 2013). To achieve rapid removal of substrates with diverse biophysical properties, robust K48-linked chain formation must be guaranteed. In contrast to a self-limiting ubiquitination in cell cycle control, ERAD employs

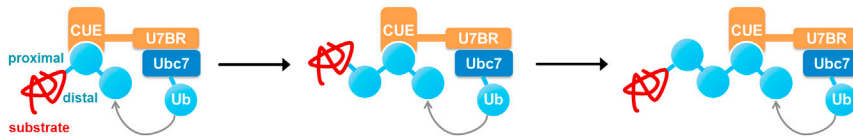


**Figure 6. Model of the Cue1-CUE Domain-Assisted Ubiquitin Chain Assembly by Ubc7**

The CUE domain of Cue1 binds single moieties of ubiquitin chains and aligns the E2 Ubc7 with the distal end of the polymer. Binding events adjacent to the acceptor ubiquitin promote chain elongation most. In addition, longer chains provide additional binding sites for CUE that further accelerate the reaction.

a self-accelerating chain assembly when Cue1 is involved. At the APC/C, the contribution of the RING domain to enhanced polyubiquitination directly connects substrate binding and ubiquitination. In contrast, Cue1/Ubc7 may represent a self-contained module adapted to quickly assemble K48-linked chains on diverse substrates in concert with different ubiquitin ligases. Recognition of certain substrate classes and their cytosolic ubiquitination seems to be disconnected at ERAD ubiquitin ligases. In the case of Hrd1, substrate recognition occurs at the ER-luminal Hrd3 domain of the ligase complex (Carvalho et al., 2006; Denic et al., 2006). This may avoid steric clashes of fixed substrates and growing chains.

Based on our results, we want to propose the following model for a UBD-mediated polyubiquitination by Ubc7 (Figure 6). In a first step, substrate proteins are ubiquitinated on one or several lysine residues. Here, contribution of the CUE domain is probably limited to shield initial modifications from deubiquitinating enzymes (Bagola et al., 2013). As soon as the substrate is primed with diubiquitin, the machinery switches to highly processive chain elongation. Cue1 binds the moiety adjacent to the acceptor ubiquitin and orients Ubc7 for ubiquitin transfer. The preference of the CUE domain for K48-linked molecules enhances this position effect and keeps the distal ubiquitin accessible. The CUE domain binds individual ubiquitin moieties with low affinity, allowing dynamic motions within the growing chain. Because the off rate of the CUE domain-ubiquitin complex is much faster than the rate of the enzymatic reaction, a higher number of binding sites within the growing chain does not inhibit the overall reaction but accelerates it by keeping the E2 in close proximity to the growing chain and, at the same time, allowing the system to sample all possible interaction positions efficiently. Although the absolute acceleration effects are relatively small (factor 2–5) compared with typical acceleration effects of enzymatic reactions with small molecules, they are within the same range as those observed for other interactions within the ubiquitin system (Metzger et al., 2013). The CUE domain enables Cue1 to act in an E4-like fashion by implementing an acceleration factor of chain elongation. Our data suggest that, in the absence of a functional CUE domain, ubiquitin chains should be formed less efficiently on specific ERAD substrates. In line with this prediction, we found that variants with reduced affinity of the CUE domain delayed proteasomal degradation of the ERAD substrate Ubc6 *in vivo*. Because Ubc6 degradation has also been shown to involve priming of the substrate with K11-linked chains, the CUE domain might also contribute to extension of K11 chains (Krefl and Hochstrasser, 2011; Xu et al., 2009). Strikingly, decelerated chain synthesis is neither compensated by downstream-acting E4 enzymes at the level of Cdc48 nor by the proteasome (Schmidt et al., 2005; Crosas et al., 2006; Jentsch and Rumpf,

2007). Hence, turnover kinetics seem to be directly defined by the efficacy of the primary ubiquitination.

## EXPERIMENTAL PROCEDURES

### Protein Purification for Structural and Interaction Studies

The codon-optimized gene of Cue1<sup>25–203</sup> and related constructs containing only the CUE domain were expressed as polyhistidine-tagged ubiquitin fusion proteins (Rogov et al., 2012). Expression was carried out in T7 Express-competent *E. coli*. Cells were grown in Luria Bertani (LB) or M9 medium and induced at 18°C for 20 hr with 0.2 mM isopropyl β-D-1-thiogalactopyranoside (IPTG). Purification included lysis, immobilized metal affinity chromatography (IMAC), tag removal by tobacco etch virus (TEV) protease, and a second IMAC step, followed by gel filtration.

To biotinylate the CUE domain, a biotinylation site was introduced between the TEV site and the coding sequence of Cue1<sup>59–115</sup>. *In vitro* biotinylation was performed in 50 mM bicine (pH 8.3), 10 mM ATP, 10 mM MgOAc, and 50 μM biotin using BirA for 1 hr at 30°C.

### Protein Expression, Purification, and Fluorescence Labeling for Functional Analysis

Ubc7, Hrd1<sup>325–551</sup> (cHrd1), Cue1<sup>25–203</sup> (cCue1), and Cue1<sup>25–203</sup> variants were cloned in a pGEX-6p1 vector, expressed and purified as described before (Bagola et al., 2013). Ube1 subcloned in a pET21d vector was produced according to a published protocol (Berndsen and Wolberger, 2011). Cdc34, Ubc13, and Uev1a in the pGEX vector were expressed and processed as reported previously (Mansour et al., 2015). The catalytic domain of the deubiquitinating enzyme Usp2 (Usp2<sub>cat</sub>) was purchased from Boston Biochem. Human ubiquitin (Ub) and all its variants, cloned in pETM60, were expressed in *E. coli* BL21 cells and produced according to previous protocols (Pickart and Raasi, 2005; Mansour et al., 2015). Labeling of cysteine-containing ubiquitin variants with the fluorescent dye Alexa Fluor 488 C5 maleimide has been described previously (Bagola et al., 2013).

### Preparative Assembly of Ubiquitin Chains

Ubiquitin chains with a proximal hexahistidine tag (6×His) were enzymatically assembled *in vitro*. K48 linkages were synthesized using Cdc34, whereas K63-linked chains were generated by Ubc13 and Uev1a. A detailed description of the reaction conditions is available in the Supplemental Experimental Procedures.

### NMR Spectroscopy

NMR experiments were performed at 298 K in NMR buffer (50 mM Na<sub>2</sub>HPO<sub>4</sub>, 100 mM NaCl [pH 7], and 5% D<sub>2</sub>O). NMR structure determination of <sup>13</sup>C-<sup>15</sup>N-labeled Cue1<sup>45–115</sup> followed a standard protocol (see Supplemental Experimental Procedures).

Titration of <sup>15</sup>N-labeled ubiquitin with CUE or <sup>15</sup>N-labeled CUE (0.2 mM) with Ub or Ub chains was monitored by [<sup>15</sup>N, <sup>1</sup>H]-heteronuclear single quantum coherence spectroscopy (HSQC) spectra. Spectra were acquired at CUE:Ub molar ratios of 0, 1/8, 1/4, 1/2, 1, 3/2, 2, 4, 8, and 16 (only in the case of monoUb titration). Because a ubiquitin chain presents multiple binding sites for CUE, the molar ratios were corrected accordingly.

The structural model of the CUE/ubiquitin complex was calculated in HADDOCK. Ambiguous interaction restraints were defined for solvent-accessible amide resonances shifting more than 0.10 ppm under saturation for CUE and 0.12 ppm for ubiquitin.

K48-Ub<sub>2</sub> (0.2 mM) and K63-Ub<sub>2</sub> (0.2 mM) carrying either a proximal or distal <sup>15</sup>N-labeled ubiquitin were titrated with unlabeled Cue1<sup>45-115</sup> up to a molar ratio of 8. To determine the K<sub>D</sub> for proximal and distal ubiquitin moieties, a fitting model for two independent binding sites with different affinities was used (Varadan et al., 2005; Wang and Jiang, 1996).

### CD Spectroscopy

CD spectroscopy experiments were performed using a JASCO J-810 spectropolarimeter in a 0.1-cm path length cuvette. Temperature-induced unfolding was monitored by ellipticity changes at 222 nm from 4°C to 90°C. Protein concentrations were adjusted to 100 μM in NMR buffer.

### In Vitro Ubiquitin Chain Elongation Reaction for Fluorescence-Based Analysis

In vitro ubiquitination reactions (performed in triplicates) modified for analysis of ubiquitin chain elongation included 0.15 μM E1 (Ube1), 2 μM Ubc7, 1.2 μM cCue1 or variants, 14.8 μM preassembled ubiquitin chains, and 0.2 μM Alexa Fluor 488-labeled Ub in fluorescence anisotropy (FA) buffer (4 mM ATP, 0.5 mM DTT, 4 mM MgCl<sub>2</sub>, and 50 mM Tris/HCl [pH 8]). Optionally 1 μM cHrd1 was added. Reactions of time-course experiments were performed in the dark at 10°C containing cHrd1 or at 20°C omitting the RING fragment. In another set of chain elongation experiments, cCue1 was crosslinked to Ub T9C, which was integrated either at the distal (K48-Ub<sub>2</sub><sup>distal</sup>~cCue1) or proximal position (K48-Ub<sub>2</sub><sup>proximal</sup>~cCue1) of diubiquitin or the proximal position of triubiquitin (K48-Ub<sub>3</sub><sup>proximal</sup>~cCue1). Crosslinking reactions with 1,8-bis(maleimido)diethylene glycol (BM(PEG)<sub>2</sub>) were carried out according to the manufacturer's manual. Conjugates were included in in vitro ubiquitination reactions and performed in triplicates. Reactions included 0.15 μM E1 (Ube1), 2 μM Ubc7, 1.2 μM cCue1 T66C C147S crosslinked to Ub T9C (in Ub<sub>2</sub> or Ub<sub>3</sub>), and 0.2 μM Alexa Fluor 488-labeled Ub in FA buffer. A similar reaction without crosslinked conjugates contained equal amounts of cCue1 and K48-Ub<sub>2</sub> (1.2 μM).

At given time points, samples were taken, and elongation was stopped using urea sample buffer. Elongation reactions monitored by fluorescence anisotropy were carried out at 20°C. Polarized emissions at 518 nm after excitation at 495 nm were measured in a spectrofluorometer (Fluoromax 4, Horiba). For subsequent deubiquitination, 500 nM Usp<sub>2cat</sub> was added after saturation of chain elongation.

Elongation products were analyzed by SDS-PAGE following fluorescence scanning employing emission filter LPB (510LP) after excitation at 473 nm and Coomassie staining.

Fluorescence intensities of elongation products were quantified using ImageQuant TL software and normalized to total fluorescence signals. Single exponential elongation kinetics were analyzed with FluorEssence software and SigmaPlot version 12, yielding kinetic rate constants of elongation reactions.

### SPR Studies

SPR experiments were performed on a Biacore X100 system. Biotinylated CUE was immobilized (~100 response units [RUs]) on a streptavidin-coated sensor chip. All experiments were carried out in buffer containing 10 mM HEPES (pH 7.4), 150 mM NaCl, 3 mM EDTA, and 0.05% Tween 20. Ub and Ub chains were injected at concentrations of 0, 2, 4, 10, 25, 50, 100, 200, 400, and 800 μM at a flow rate of 50 μl/min (100 s injections). In the case of polyubiquitin chains, the concentrations were adjusted according to the number of ubiquitin molecules. Dissociation constants were calculated using BIAevaluation software from control-corrected, steady-state RUs. This yielded apparent dissociation constants for a single ubiquitin within a chain under the assumption that all binding sites are equal.

### Cycloheximide Decay Assay

Protein degradation was analyzed in yeast cells by means of blocking translation. Forty milliliters of cells in log phase (OD<sub>600</sub> = 0.6) were suspended in synthetic defined (SD) medium containing 0.35 mg/mL cycloheximide and incubated at 30°C. A total of 500 μL of ice-cold 30 mM Na<sub>2</sub>S<sub>2</sub>O<sub>8</sub> and 1 mM PMSF stopped degradation after 1, 2, and 3 hr. Cells were lysed by glass beads and strong agitation in 50 mM Tris/HCl (pH 7.5), 1% (w/v) SDS, and

1 mM PMSF. Ubc6, Sec61, and Cue1 were analyzed by SDS-PAGE and western blotting according to Bagola et al. (2013).

### ACCESSION NUMBERS

The accession number for the CUE domain structure reported in this paper is PDB: 2MYX.

### SUPPLEMENTAL INFORMATION

Supplemental Information includes Supplemental Experimental Procedures, seven figures, and one table and can be found with this article online at <http://dx.doi.org/10.1016/j.molcel.2016.04.031>.

### AUTHOR CONTRIBUTIONS

M.v.D. and A.K. designed and performed experiments and wrote the manuscript. V.V.R. and F.L. performed the NMR experiments, P.G. conducted the structure calculation, and K.B. and L.P. generated constructs, wrote the manuscript, and performed experiments. V.V.R., T.S., and V.D. guided the project planning and wrote the manuscript.

### ACKNOWLEDGMENTS

The authors thank Prof. C. Wolberger for Ube1 subcloned in a pET21d vector and all members of the V.D. and T.S. research group, especially E. Jarosch, for unpublished data, materials, and discussions. This work was funded by the Deutsche Forschungsgemeinschaft (SFB 740, Priority Program 1365), the Deutsch-Israelische Projektkooperation (DIP), the LOEWE program, Ubiquitin Networks, and the Cluster of Excellence Frankfurt (Macromolecular Complexes). P.G. is supported by a Lichtenberg professorship of the Volkswagen Foundation.

Received: December 28, 2015

Revised: March 21, 2016

Accepted: April 25, 2016

Published: June 2, 2016

### REFERENCES

- Bagola, K., von Delbrück, M., Dittmar, G., Scheffner, M., Ziv, I., Glickman, M.H., Ciechanover, A., and Sommer, T. (2013). Ubiquitin binding by a CUE domain regulates ubiquitin chain formation by ERAD E3 ligases. *Mol. Cell* 50, 528–539.
- Bays, N.W., Gardner, R.G., Seelig, L.P., Joazeiro, C.A., and Hampton, R.Y. (2001). Hrd1p/Der3p is a membrane-anchored ubiquitin ligase required for ER-associated degradation. *Nat. Cell Biol.* 3, 24–29.
- Bazirgan, O.A., and Hampton, R.Y. (2008). Cue1p is an activator of Ubc7p E2 activity in vitro and in vivo. *J. Biol. Chem.* 283, 12797–12810.
- Berndsen, C.E., and Wolberger, C. (2011). A spectrophotometric assay for conjugation of ubiquitin and ubiquitin-like proteins. *Anal. Biochem.* 418, 102–110.
- Biederer, T., Volkwein, C., and Sommer, T. (1997). Role of Cue1p in ubiquitination and degradation at the ER surface. *Science* 278, 1806–1809.
- Brown, N.G., Watson, E.R., Weissmann, F., Jarvis, M.A., VanderLinden, R., Grace, C.R., Frye, J.J., Qiao, R., Dube, P., Petzold, G., et al. (2014). Mechanism of polyubiquitination by human anaphase-promoting complex: RING repurposing for ubiquitin chain assembly. *Mol. Cell* 56, 246–260.
- Brzovic, P.S., Lissounov, A., Christensen, D.E., Hoyt, D.W., and Klevit, R.E. (2006). A UbcH5/ubiquitin noncovalent complex is required for processive BRCA1-directed ubiquitination. *Mol. Cell* 21, 873–880.
- Buetow, L., Gabrielsen, M., Anthony, N.G., Dou, H., Patel, A., Aitkenhead, H., Sibbet, G.J., Smith, B.O., and Huang, D.T. (2015). Activation of a primed RING E3-E2-ubiquitin complex by non-covalent ubiquitin. *Mol. Cell* 58, 297–310.

- Carvalho, P., Goder, V., and Rapoport, T.A. (2006). Distinct ubiquitin-ligase complexes define convergent pathways for the degradation of ER proteins. *Cell* 126, 361–373.
- Chen, Z.J., and Sun, L.J. (2009). Nonproteolytic functions of ubiquitin in cell signaling. *Mol. Cell* 33, 275–286.
- Choi, Y.-S., Wu, K., Jeong, K., Lee, D., Jeon, Y.H., Choi, B.-S., Pan, Z.-Q., Ryu, K.-S., and Cheong, C. (2010). The human Cdc34 carboxyl terminus contains a non-covalent ubiquitin binding activity that contributes to SCF-dependent ubiquitination. *J. Biol. Chem.* 285, 17754–17762.
- Choi, Y.-S., Lee, Y.-J., Lee, S.-Y., Shi, L., Ha, J.-H., Cheong, H.-K., Cheong, C., Cohen, R.E., and Ryu, K.-S. (2015). Differential ubiquitin binding by the acidic loops of Ube2g1 and Ube2r1 enzymes distinguishes their Lys-48-ubiquitylation activities. *J. Biol. Chem.* 290, 2251–2263.
- Conaway, R.C., Brower, C.S., and Conaway, J.W. (2002). Emerging roles of ubiquitin in transcription regulation. *Science* 296, 1254–1258.
- Crosas, B., Hanna, J., Kirkpatrick, D.S., Zhang, D.P., Tone, Y., Hathaway, N.A., Buecker, C., Leggett, D.S., Schmidt, M., King, R.W., et al. (2006). Ubiquitin chains are remodeled at the proteasome by opposing ubiquitin ligase and deubiquitinating activities. *Cell* 127, 1401–1413.
- de Vries, S.J., van Dijk, M., and Bonvin, A.M. (2010). The HADDOCK web server for data-driven biomolecular docking. *Nat. Protoc.* 5, 883–897.
- Denic, V., Quan, E.M., and Weissman, J.S. (2006). A luminal surveillance complex that selects misfolded glycoproteins for ER-associated degradation. *Cell* 126, 349–359.
- Foresti, O., Rodriguez-Vaello, V., Funaya, C., and Carvalho, P. (2014). Quality control of inner nuclear membrane proteins by the Asi complex. *Science* 346, 751–755.
- Haglund, K., and Dikic, I. (2005). Ubiquitylation and cell signaling. *EMBO J.* 24, 3353–3359.
- Huang, T.T., and D’Andrea, A.D. (2006). Regulation of DNA repair by ubiquitylation. *Nat. Rev. Mol. Cell Biol.* 7, 323–334.
- Husnjak, K., and Dikic, I. (2012). Ubiquitin-binding proteins: decoders of ubiquitin-mediated cellular functions. *Annu. Rev. Biochem.* 81, 291–322.
- Jentsch, S., and Rumpf, S. (2007). Cdc48 (p97): a “molecular gearbox” in the ubiquitin pathway? *Trends Biochem. Sci.* 32, 6–11.
- Kang, R.S., Daniels, C.M., Francis, S.A., Shih, S.C., Salerno, W.J., Hicke, L., and Radhakrishnan, I. (2003). Solution structure of a CUE-ubiquitin complex reveals a conserved mode of ubiquitin binding. *Cell* 113, 621–630.
- Kelly, A., Wickliffe, K.E., Song, L., Fedrigo, I., and Rape, M. (2014). Ubiquitin chain elongation requires E3-dependent tracking of the emerging conjugate. *Mol. Cell* 56, 232–245.
- Khmelniskii, A., Blaszcak, E., Pantazopoulou, M., Fischer, B., Omnus, D.J., Le Dez, G., Brossard, A., Gunnarsson, A., Barry, J.D., Meurer, M., et al. (2014). Protein quality control at the inner nuclear membrane. *Nature* 516, 410–413.
- Koegl, M., Hoppe, T., Schlenker, S., Ulrich, H.D., Mayer, T.U., and Jentsch, S. (1999). A novel ubiquitination factor, E4, is involved in multiubiquitin chain assembly. *Cell* 96, 635–644.
- Komander, D., and Rape, M. (2012). The ubiquitin code. *Annu. Rev. Biochem.* 81, 203–229.
- Kostova, Z., Mariano, J., Scholz, S., Koenig, C., and Weissman, A.M. (2009). A Ubc7p-binding domain in Cue1p activates ER-associated protein degradation. *J. Cell Sci.* 122, 1374–1381.
- Kreft, S.G., and Hochstrasser, M. (2011). An unusual transmembrane helix in the endoplasmic reticulum ubiquitin ligase Doa10 modulates degradation of its cognate E2 enzyme. *J. Biol. Chem.* 286, 20163–20174.
- Kreft, S.G., Wang, L., and Hochstrasser, M. (2006). Membrane topology of the yeast endoplasmic reticulum-localized ubiquitin ligase Doa10 and comparison with its human ortholog TEB4 (MARCH-VI). *J. Biol. Chem.* 281, 4646–4653.
- Liu, S., Chen, Y., Li, J., Huang, T., Tarasov, S., King, A., Weissman, A.M., Byrd, R.A., and Das, R. (2012). Promiscuous interactions of gp78 E3 ligase CUE domain with polyubiquitin chains. *Structure* 20, 2138–2150.
- Mansour, W., Nakasone, M.A., von Delbrück, M., Yu, Z., Krutauz, D., Reis, N., Kleifeld, O., Sommer, T., Fushman, D., and Glickman, M.H. (2015). Disassembly of Lys11 and mixed linkage polyubiquitin conjugates provides insights into function of proteasomal deubiquitinases Rpn11 and Ubp6. *J. Biol. Chem.* 290, 4688–4704.
- Metzger, M.B., Liang, Y.-H., Das, R., Mariano, J., Li, S., Li, J., Kostova, Z., Byrd, R.A., Ji, X., and Weissman, A.M. (2013). A structurally unique E2-binding domain activates ubiquitination by the ERAD E2, Ubc7p, through multiple mechanisms. *Mol. Cell* 50, 516–527.
- Meyer, H.-J., and Rape, M. (2014). Enhanced protein degradation by branched ubiquitin chains. *Cell* 157, 910–921.
- Pastushok, L., Moraes, T.F., Ellison, M.J., and Xiao, W. (2005). A single Mms2 “key” residue insertion into a Ubc13 pocket determines the interface specificity of a human Lys63 ubiquitin conjugation complex. *J. Biol. Chem.* 280, 17891–17900.
- Pickart, C.M., and Raasi, S. (2005). Controlled synthesis of polyubiquitin chains. *Methods Enzymol.* 399, 21–36.
- Ravid, T., and Hochstrasser, M. (2007). Autoregulation of an E2 enzyme by ubiquitin-chain assembly on its catalytic residue. *Nat. Cell Biol.* 9, 422–427.
- Rogov, V.V., Rozenknop, A., Rogova, N.Y., Löhr, F., Tikole, S., Jaravine, V., Güntert, P., Dikic, I., and Dötsch, V. (2012). A universal expression tag for structural and functional studies of proteins. *ChemBioChem* 13, 959–963.
- Schmidt, M., Hanna, J., Elsasser, S., and Finley, D. (2005). Proteasome-associated proteins: regulation of a proteolytic machine. *Biol. Chem.* 386, 725–737.
- Thrower, J.S., Hoffman, L., Rechsteiner, M., and Pickart, C.M. (2000). Recognition of the polyubiquitin proteolytic signal. *EMBO J.* 19, 94–102.
- Varadan, R., Assfalg, M., Raasi, S., Pickart, C., and Fushman, D. (2005). Structural determinants for selective recognition of a Lys48-linked polyubiquitin chain by a UBA domain. *Mol. Cell* 18, 687–698.
- Wang, Z.X., and Jiang, R.F. (1996). A novel two-site binding equation presented in terms of the total ligand concentration. *FEBS Lett.* 392, 245–249.
- Weissman, A.M. (2001). Themes and variations on ubiquitylation. *Nat. Rev. Mol. Cell Biol.* 2, 169–178.
- Wickliffe, K.E., Lorenz, S., Wemmer, D.E., Kuriyan, J., and Rape, M. (2011). The mechanism of linkage-specific ubiquitin chain elongation by a single-subunit E2. *Cell* 144, 769–781.
- Wright, J.D., Mace, P.D., and Day, C.L. (2016). Secondary ubiquitin-RING docking enhances Arkadia and Ark2C E3 ligase activity. *Nat. Struct. Mol. Biol.* 23, 45–52.
- Xu, P., Duong, D.M., Seyfried, N.T., Cheng, D., Xie, Y., Robert, J., Rush, J., Hochstrasser, M., Finley, D., and Peng, J. (2009). Quantitative proteomics reveals the function of unconventional ubiquitin chains in proteasomal degradation. *Cell* 137, 133–145.